

DESIGN AND INITIAL OPERATION OF MULTICHORD SOFT X-RAY DETECTION ARRAY ON THE U-3M TORSATRON

M.B. Dreval

Institute of Plasma Physics NSC KIPT, Kharkov, Ukraine

A miniature pinhole camera array for spatially and temporally resolved measurements of soft X-ray emission has been designed and installed in the URAGAN-3M torsatron. Two features of the U-3M: a) very large vacuum vessel; b) a quite high RF noise from the 8-9 MHz plasma heating generators, form a rather difficult for the SXR system design conditions. In order to increase the SXR brightness in 25-50 times the pinhole camera is placed between helical coils near plasma in the "A-A" cross-section. The size of the pinhole and its location relative to the diode array are optimized to cover the whole poloidal cross section and to achieve a good spatial resolution with minimum overlap in nearby channels. Possible misalignments of the SXR system can cause errors in the line of sight impact parameter less than 3^0 (similar to the SXR channel viewing angle). The maximum of the measured SXR brightness intensity corresponds to the central channel № 11 of the system. The $2.5 \cdot 10^7$ V/A SXR photodiode photocurrent amplifiers with additional RF noise suppress electronics have been manufactured. The SXR electronics does successfully work in high vacuum conditions near the plasma. Time evolution of the SXR emission profile and its fluctuations are successfully measuring by the designed diagnostics.

PACS: 52.55.Hc; 52.70.La

INTRODUCTION

Soft X-ray (SXR) diagnostics is an important tool for studies various phenomena in fusion plasmas. The diagnostics are used to study a variety of phenomena, such as MHD activity [1-3], toroidicity-induced Alfvén eigenmodes (TAE) etc. Relative simplicity and low cost of the SXR diagnostics (in comparison with the electron cyclotron emission and the Thomson scattering diagnostics) in addition to its high performance determine its wide application at tokamaks, stellarators, reverse field pinches, etc [1-3]. Due to lack of diagnostics, described in this work multichannel SXR pinhole camera array is almost unique tool (in addition to the multichannel H_α monitoring) available in U-3M for a plasma profile monitoring and internal plasma fluctuations studies based on single discharge data.

A 1.5 m distance from U-3M chamber wall to the plasma is formed by the "chamber-less" U-3M design. Such a long distance defines significant SXR brightness decay (proportional to the square of this distance). Initially designed for the U-2M torsatron [4] the SXR diagnostics has been adopted for rather unusual U-3M conditions. In order to increase the SXR brightness in 25-50 times the pinhole camera is placed between helical coils near the plasma. A set of design features related to such a decision as well as related to a strong 8-9MHz load from the U-3M radio frequency (RF) heating generators are described in this work.

In order to increase SXR signal strength and remain its appropriate spatial resolution the SXR pinhole camera design optimization has been performed in the present work. The optimization take place for the U-3M stellarator geometry in condition of non-circular rotated in toroidal direction magnetic surfaces. A possible misalignment of the SXR system geometry is discussed.

1. SXR, PASSED THROUGH 2 μm Al FOIL

On the base of previous estimations [4], in order to increase signal amplitude a thin 2 μm Al foil was installed on the U-3M SXR pinhole slit. Soft X-ray

emission in the plasma includes free-bound recombination radiation; the bound-bound line radiation introducing photons in the low energy range. In order to get information about the measured SXR signal for just qualitative estimations, let's consider the continuum emission only, which is expressed by the bremsstrahlung formula for a Maxwellian plasma:

$$\frac{dW}{dE} \propto n_e(r)n_i(r)Z_{\text{eff}}^2(r)T_e^{-0.5}(r)e^{-\frac{E}{T_e(r)}}, \quad \text{where}$$

dW is the radiation power emitted in the photon energy interval dE and n_e , n_i , Z_{eff} , and T_e are electron and ion density, effective plasma charge and electron temperature, respectively. The SXR intensity in a detector is defined by integrated along line of sight l and photon energies E SXR emitted by plasma. Its filtering by a foil leads to the following SXR intensity in the detector:

$$I \propto \int_l \frac{n_e^2(l)}{\sqrt{T_e(l)}} \int_E \exp\left[-\frac{E}{T_e(l)}\right] \exp\left[-\frac{\mu}{\rho}(E)\rho \cdot t\right] dE dl,$$

where μ/ρ is the mass energy absorption coefficient of a foil. The temperature dependence of the SXR signal in the case of 2 μm Al filter is shown in Fig. 1. The dependence was obtained by numerical integration using recent μ/ρ data, as it is described in [4]. The photodiode array IRD AXUV-20EL, used as a detector part, has almost flat energy dependence in the 0.2...4000 eV photon energy range. Thus, the calculated temperature dependence is not significantly disturbed in the 0.25...1 keV temperature range.

2. GEOMETRICAL DESIGN

The SXR camera array consists of a 20 channel photodiode linear array, a shielding box, electronics and a pinhole. The front cover of the detector consists of two flat plates having pinholes in the middle. The Al foil is clamped between the plates. The size of the pinhole and its location relative to the diode array are optimized to cover the whole poloidal cross section and to achieve a good spatial resolution with minimum overlap of

nearby channels, as it is described below. Each IRD AXUV-20EL array contains 20 rectangular photodiodes, each having a sensitive area of 0.75×4 mm and an active thickness of $35 \mu\text{m}$. The SXR camera consists of 20 fanlike lines of sight. The camera is viewing horizontally through a symmetric plasma cross section "A-A", as it is shown in Fig. 2. This U-3M cross section is selected as a longest one in the vertical direction. Large vertical plasma size determines better space resolution of the diagnostics and allows use big enough poloidal collecting angle, maintaining high enough SXR signal.

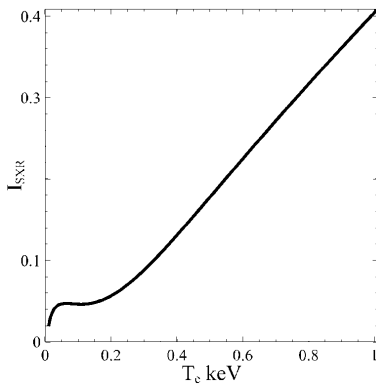


Fig. 1. SXR emission, passed from $2 \mu\text{m}$ Al foil

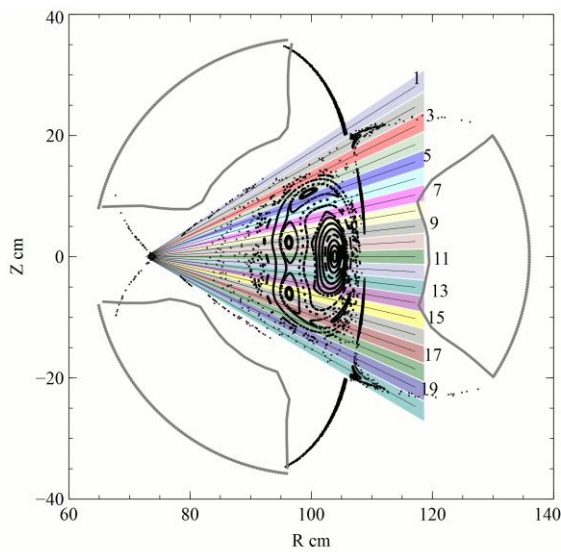


Fig. 2. Lines of sight and viewing angles of the SXR detector arrays across the cross section "A-A"

The pinhole camera geometry defines the poloidal viewing area of SXR channels as shown in Fig. 3. The observation angle for any point on the photon sensitive area is 3° in the poloidal direction. Due to the finite size of the sensitive area, the total viewing angle of each sensitive element is about 6° .

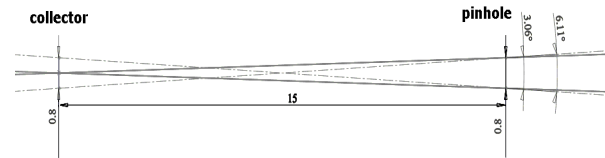


Fig. 3. Viewing angles of pinhole camera channels used on U-3M (the unit of the linear lengths is in millimeters)

Fig. 2 shows the viewing angles (3°) of the channels of an SXR array used for the U-3M torsatron. Wide enough toroidal viewing angles have been selected for the signal amplitude increase, as it is shown in Fig. 4.

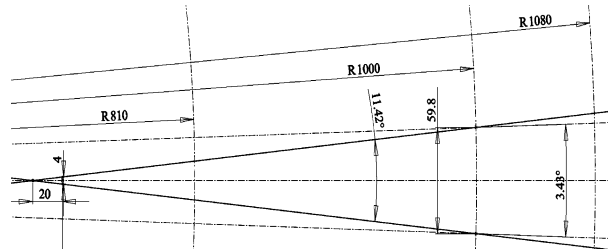


Fig. 4. Viewing angles in the toroidal plane (the unit of the linear lengths is in millimeters)

A toroidal divergence of the viewing angle causes an artificial widening of the spatial resolution in the poloidal plane due to the magnetic surfaces rotation. The toroidal viewing angle of 11.4° corresponds to the angle between marginal cross-sections defined by toroidal widening about 4° . A central magnetic surfaces cross-section (A-A) and turned on $\pm 2^\circ$ are shown in Fig. 5.

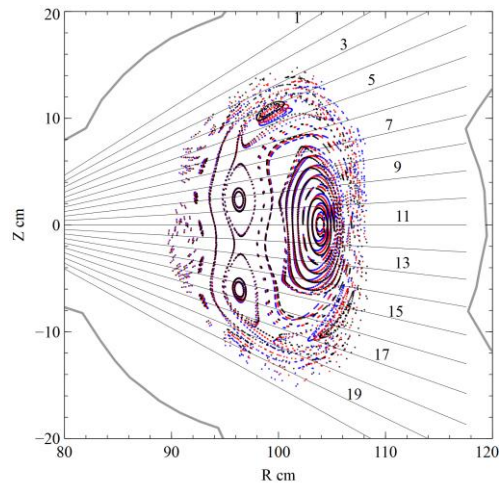


Fig. 5. Lines of sight and magnetic surfaces in the A-A (black color) and $\pm 2^\circ$ turned U-3M cross-sections

The spatial resolution restriction due the toroidal divergence of the viewing area is significantly lower in comparison with the poloidal one, as it is clear from the figures. Fig. 6 shows a photograph of the SXR detector array installed between helical coils of the U-3M.



Fig. 6. SXR diagnostics installed between helical coils

The detector box is fixed to a curved helical coils cover, what can cause misalignments. Due to short distance from the detector to plasma, possible toroidal misalignments in $3...5^\circ$ would cause rotation of “seen” magnetic surfaces only in 1° , as it was shown above. Thus, toroidal misalignments can be neglected. An influence of possible displacement of the detector in the radial direction is shown in Fig. 7.

Real accuracy of the radial position of the detector is about $\pm 1\text{cm}$, but even in a case of $\pm 2\text{ cm}$ displacement, modification of the impact parameter of the lines of sight is not higher than the poloidal viewing angles width.

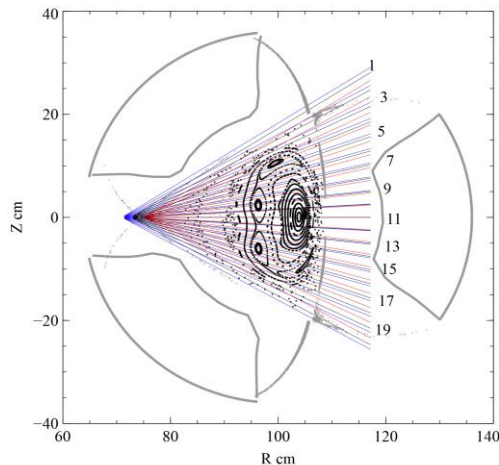


Fig. 7. Lines of sight in case of $\pm 2\text{ cm}$ displacement

3. ELECTRONICS DESIGN

AXUV-20EL photodiodes have flat response over a wide range from visible light to x-ray and are therefore also suitable for bolometric measurements. High responsivity of 0.275 A/W , low noise and 200 ns risetime allow AXUV-20EL applications in high speed SXR systems. Precision, low noise, 10MHz bandwidth, small size operational amplifier AD8606 has been selected for SXR diode current preamplifiers. Two stages of SXR photodiode photocurrent amplifiers with fixed combined gains of $2.5 \cdot 10^7\text{ V/A}$ have been manufactured. The preamplifiers are placed near the diode assembly in a vacuum. The SXR electronics does successfully work in high vacuum conditions near the plasma due to heat sink optimization, as well as due to

stainless steel shielding from the plasma. RLC filters with a ferrite beads inserted in an output stage of the amplifiers prevent a noise pick-up by the output cables. Similar filters and voltage regulators prevent pulsations of the supply and bias voltages. The amplifiers bandwidth decrease down to 10 kHz , what allows to suppress successfully high RF noise and to register SXR signals. Low cost, 12 bit resolution, 16 channels, up to 8 MS/s sampling rate, 1 MS/channel on board memory TEREX ET-1255 ADC board is used for the SXR diagnostics.

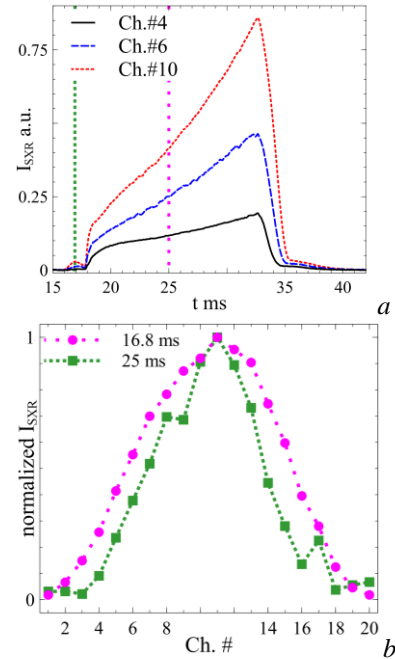


Fig. 8. Time evolution (a) and SXR signal distributions (b) versus channel number in two moments of RF discharge

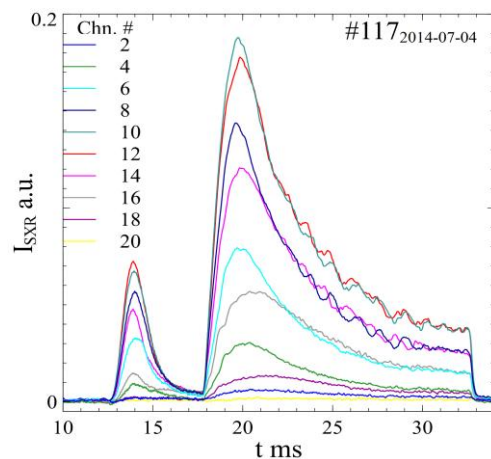


Fig. 9. An example of the SXR fluctuations

4. FIRST RESULTS

Possible SXR camera misalignment in the poloidal direction can be verified by an experimental data. A maximum of the SXR emissivity is expected from a line crossing plasma center. Time evolution of SXR emissivity of channels № 4, 6 and 10 and SXR emissivity dependence on the channel number are

shown in Fig. 8. As shown in the figure, the maximum of the measured SXR brightness intensity corresponds to the central channel № 11 of the system.

This maximum location is always observed in normal U-3M discharges. Therefore, a difference between designed lines of sight geometry (see in the Fig. 2) and real geometry is not significant and possible error in the impact parameter is less than 3^0 poloidal viewing angle of the SXR channel.

The installed SXR system bandwidth is limited for the noise suppression purpose. Only low frequency fluctuations can be measured at the present time. Various fluctuations of the U-3M SXR emission have been observed in a frequency range about few kilohertz or less. An example of the fluctuations is shown in Fig. 9. Clear localization of the fluctuations in a central region and its absence in the edge channels in the discharge № 117 evidently show that it is not a noise. The fluctuation phase inversion is observed in symmetric lines of sight with opposite sign of its impact parameters (like channel № 8 and № 14). Different types of fluctuations, without the phase inversion and

with different spatial localizations are observed in different types of the U-3M discharge as well.

ACKNOWLEDGEMENTS

This work was supported by the STSU project 4216. Technical support provided by Mr. S.M. Maznichenko and the IPP Machine Shop is gratefully acknowledged.

REFERENCES

1. M. Dreval, et al. // *Rev. Sci. Instrum.* 2011, v. 82, p. 053503.
2. M. Dreval et al. // *Radiation Effects & Defects in Solids.* 2011, v. 166, p. 765.
3. P. Franz, L. Marrelli, et al. // *Phys. Rev. Lett.* 2004, v. 92, p. 125001.
4. M. Dreval. // *Probl. Atom. Sci. Technol.* 2010 v. 6, p. 11.
5. <http://www.ird-inc.com>

Article received 20.09.2014

РАЗРАБОТКА И НАЧАЛЬНАЯ РАБОТА МНОГОХОРДОВОГО МНОГОКАНАЛЬНОГО ДЕТЕКТОРА МЯГКОГО РЕНТГЕНА ДЛЯ ТОРСАТРОНА У-3М

М.Б. Древаль

Миниатюрный датчик для измерения временного поведения и пространственного распределения излучения мягкого рентгена был спроектирован и установлен на торсатроне УРАГАН-3М (У-3М). Две особенности У-3М: а) очень большой вакуумный объём; б) очень большой ВЧ-шум от 8-9 МГц-генераторов, нагревающих плазму, формируют очень сложные условия для проектировки диагностики мягкого рентгена. Для того, чтобы увеличить измеряемую светимость рентгена в 25-50 раз, измеряющая рентген камера обскура помещена между винтовыми проводниками рядом с плазмой в сечении "А-А". Размер входной щели и её расстояние до набора фотодиодов камеры обскуры оптимизированы для покрытия всего полоидального сечения плазмы и получения хорошего пространственного разрешения при минимальном перекрытии соседних каналов. Проведённые оценки показали, что возможные перекосы камеры могут вызвать ошибку в определении прицельного параметра хорды наблюдения меньше, чем величина угла обзора канала мягкого рентгена, в 3^0 . Максимум измеряемой интенсивности светимости мягкого рентгена приходится на центральный канал № 11. Изготовлены усилители фототока чувствительностью $2,5 \cdot 10^7$ В/А с дополнительной электроникой, подавляющей ВЧ-шум. Электроника успешно работает в условиях высокого вакуума рядом с плазмой. Временная эволюция профиля эмиссии мягкого рентгена и её флуктуаций успешно измеряются разработанной диагностикой.

РОЗРОБКА ТА НАЧАЛЬНА РОБОТА МНОГОХОРДОВОГО БАГАТОКАНАЛЬНОГО ДЕТЕКТОРА М'ЯКОГО РЕНТГЕНА ДЛЯ ТОРСАТРОНУ У-3М

М.Б. Древаль

Мініатюрний датчик для вимірювання часового поведіння та просторового розподілу випромінювання м'якого рентгена був спроектований і встановлений на торсатроні УРАГАН-3М (У-3М). Дві особливості У-3М: а) дуже великий вакуумний об'єм; б) дуже великий ВЧ-шум від 8-9 МГц-генераторів, що нагрівають плазму, формують дуже складні умови для проектування діагностики м'якого рентгена. Для того, щоб збільшити світність рентгена, що вимірюється, в 25-50 разів, камера обскура поміщена між гвинтовими проводниками поруч з плазмою у перерізі "А-А". Розмір входної щілини і її відстань до набору фотодіодів камери обскура оптимізовані для покриття всього полоїдального перерізу плазми і отримання доброго просторового розділення при мінімальному перекритті сусідніх каналів. Проведені оцінки показали, що можливі перекося камери можуть викликати помилку у визначенні прицільного параметра хорди спостереження менше, ніж величина кута огляду каналу м'якого рентгена, в 3^0 . Максимум вимірюваної інтенсивності світності м'якого рентгена припадає на центральний канал № 11. Виготовлені підсилювачі фотоструму чутливістю $2,5 \cdot 10^7$ В/А з додатковою електронікою, що переважає ВЧ-шум. Електроніка успішно працює в умовах високого вакууму поруч з плазмою. Часова еволюція профілю емісії м'якого рентгена і її флуктуацій успішно вимірюються розробленою діагностикою.